

The route of random process to ultraslow aging phenomena

Chunyan Li,¹ Haiwen Liu,^{1,2,*} and X. C. Xie^{2,3,4}

¹Center for Advanced Quantum Studies, Department of Physics, Beijing Normal University, Beijing 100875

²Interdisciplinary Center for Theoretical Physics and Information Sciences, Fudan University, Shanghai 200433, China

³International Center for Quantum Materials, School of Physics, Peking University, Beijing 100871, China

⁴Hefei National Laboratory, Hefei 230088, China

Logarithmic aging phenomena are prevalent in various systems, including electronic materials and biological structures. This study utilizes a generalized continuous-time random walk (CTRW) framework to investigate the mechanisms behind the logarithmic aging phenomena. By incorporating non-Markovian jump processes with significant memory effects, we modify traditional diffusion models to exhibit logarithmic decay in both survival and return probabilities. In addition, we analyze the impact of aging on autocorrelation functions, illustrating how long-term memory behaviors affect the temporal evolution of physical properties. These results connect microscopic models to macroscopic manifestations in real-world systems, advancing the understanding of ultraslow dynamics in disordered systems.

Logarithmic aging phenomena have been ubiquitously observed across a spectrum of complex systems, including conductance relaxations in Anderson insulators and electron glasses [1, 2], the evolution of frictional strength [3], the dynamics of compaction in granular systems [4], flux-creep dynamics in superconductors [5], and logarithmic kinetics in various glassy systems [6–8], as well as in the structural relaxation processes of proteins and DNA [9–11]. A substantial body of theoretical and phenomenological research [4, 12–15] supports these observations. Understanding the underlying mechanisms of ultraslow aging phenomena is crucial for predicting the long-term behavior of complex systems and improving the design of materials and devices with enhanced stability and performance.

Previously, Lomholt et al. [16] have enhanced our comprehension by developing a microscopic model of log-aging diffusion, which extends the Continuous Time Random Walk [17–19] (CTRW) framework by incorporating non-renewal processes. Commonly, normal diffusion is characterized by a waiting time with a finite mean time, while subdiffusion [20–22] is distinguished by a waiting time distribution with a prolonged tail. Meanwhile, the timing of subsequent events in subdiffusion, influenced by the observation time t_a , is modeled using the forward waiting time distribution $\psi_1(t, t_a)$ [23, 24]. To address the enhanced memory effect, Lomholt et al. [16] adeptly adopted the waiting time distribution with functional form identical to $\psi_1(t, t_a) = \frac{\sin \pi \alpha}{\pi} \frac{t_a^\alpha}{t^\alpha (t+t_a)}$ of the subdiffusion. This conceptual advancement gives rise to ultraslow kinetics $\langle n \rangle \sim \frac{1}{u(\alpha)} \ln(t/t_0)$, where $\langle n \rangle$ represents the ensemble average of jump steps and t_0 is the initial time exerting an external perturbation, $u(\alpha) = -\gamma - \partial \ln \Gamma(\alpha) / \partial \alpha$. This non-renewable log-aging process can be effectively demonstrated, using the analogy of a passenger’s increasingly restricted mobility over time due to the subdiffusive nature of bus arrivals, as illustrated in Fig. 1A. Although these innovative correlations between jump steps and time have garnered significant

attention [25, 26], actualizing these models into measurable real-world phenomena continues to pose significant challenges.

Investigation of the target problem, involving a stationary target surrounded by one or more random walkers, is crucial in diverse disciplines, including relaxation dynamics in polymeric systems and glasses [27–29], complex networks [30, 31], and molecular navigation within biological cells [32]. We derive the survival probability of the target under log-aging diffusion as a function of $\ln(t/t_0)$ (Fig. 1B), elucidating the logarithmically slow decay observed in electron glass of Anderson insulators [2]. Furthermore, we examine the returning probability $P(x=0, t)$, assessable via fluorescence spectroscopy, and demonstrate its dependence on time as $P(x=0, t) \sim \sqrt{\frac{u(\alpha)}{\ln(t/t_0)}}$ (see Fig. 1C). Importantly, we provide a time matching transformation between internal time and laboratory time to unify the normal, subdiffusive, and log-aging diffusion processes.

The log-aging diffusion significantly impacts system dynamics by inducing enhanced memory capabilities. The autocorrelation function emerges as an essential physical quantity for characterizing the relaxation properties of glass systems [33–36], and has garnered substantial interest in the field of biology [37, 38]. Previous research [39] utilizing single-particle tracking experiments has identified that the position autocorrelation function, $C_x = \langle x(t)x(0) \rangle$, exhibits slow decay in autocorrelation of subdiffusion described by a generalized Langevin equation. Our investigations reveal that the position autocorrelation function for the log-aging diffusion is given by $C_x \sim \left(\frac{t_0}{t}\right)^{\frac{k}{u(\alpha)}}$, with k denoting a constant irrelevant to the random process, as shown in Fig. 1D, presenting a remarkable ultraslow behavior compared to subdiffusion.

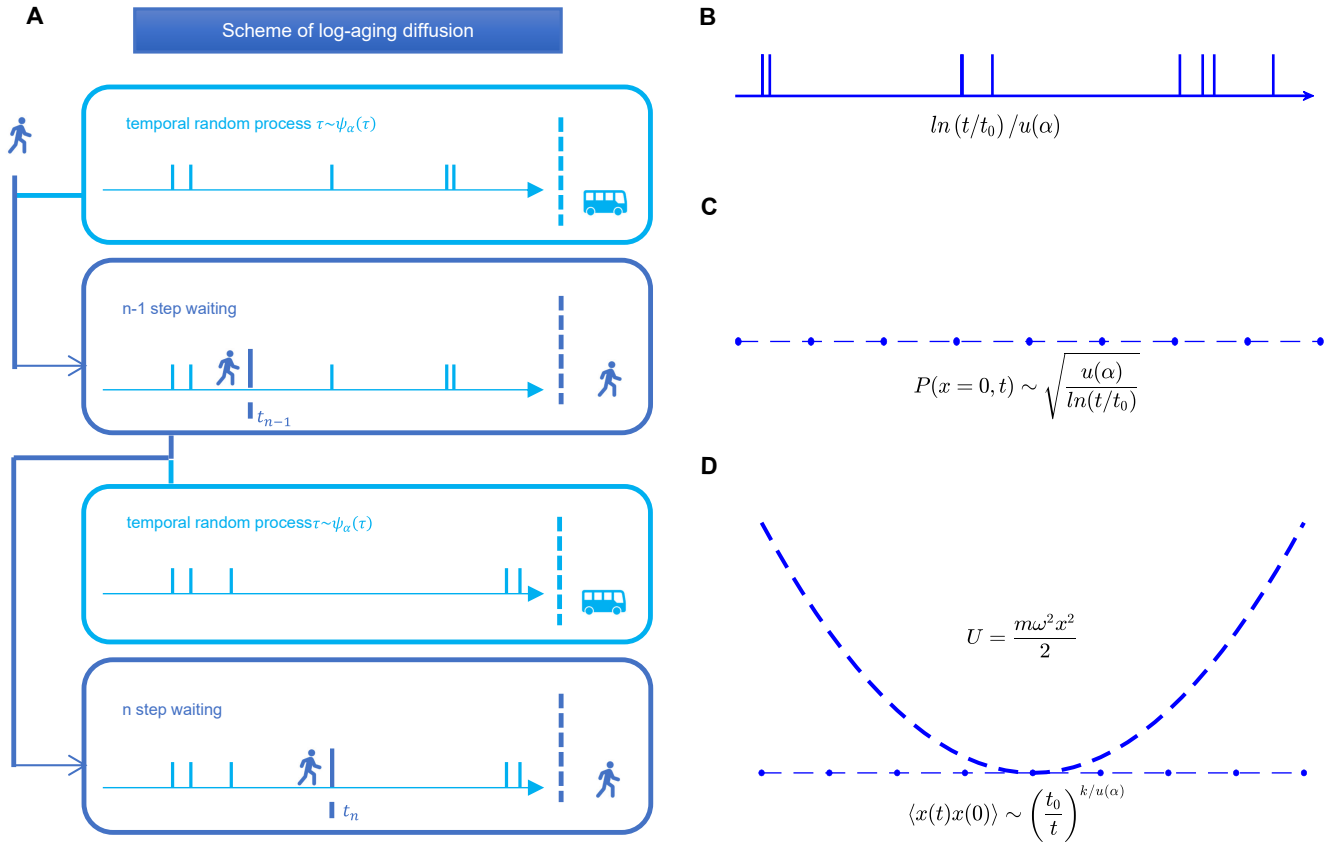


FIG. 1. Scheme and characteristics of log-aging diffusion. (A), We present a log-aging diffusion process, using a scenario where a passenger is waiting to board a bus. The intervals between bus departures at each stop are modeled by a long-tail distribution, expressed as $\psi_\alpha \sim \frac{1}{t^{1+\alpha}}$. Upon the passenger's arrival at the $n-1$ stop, they encounter a wait of t_{n-1} . Once the immediate bus arrives at the $n-1$ stop, the passenger boards swiftly and proceeds to the next stop n with the travel time considerably shorter than the waiting time. Upon reaching stop n , the passenger waits for the next bus, timing the wait as t_n . (B), Displayed are the first nine states of a particle undergoing the diffusion process described in (A), parameterized by $\alpha = 0.6$, $t_0 = 10^3$. We define $u(\alpha) = -\gamma - \partial \ln \Gamma(\alpha) / \partial \alpha$, where γ is the Euler constant and Γ is complete gamma function. (C), The return probability without external forces for the log-aging diffusion is computed as $P(x=0, t)$. (D), The positional autocorrelation function under the influence of an oscillator potential is given, $C_x = \langle x(t)x(0) \rangle$.

LOGARITHMIC RELAXATION THROUGH LOG-AGING PROCESS

The slow kinetics inherent to CTRW significantly influence the physical observables. A notable manifestation of this is the Williams-Watts form of relaxation, which can be derived from a CTRW characterized by a long-tail pausing-time distribution [40]. Furthermore, Montroll et al. [40] elucidated a profound link between various relaxation processes, such as current decay and dielectric function, and survival probability, the likelihood of mobile defects evading traps. Specifically, the Williams-Watts-type relaxation function correlates with the survival probability of mobile defects in 1D lattice undergoing subdiffusion as follows:

$$\phi(t) \sim 1 - \frac{k_1}{L} t^{\alpha/2} \sim e^{-c \cdot k_1 \cdot t^{\alpha/2}}, \quad (1)$$

where k_1 is a function of α , L represents the length of a 1D lattice, the second expression details the survival probability of a single defect, and the final expression models the survival probability of N defects with density $c = \frac{N}{L}$. However, despite the prevalence of the Williams-Watts type relaxation function across various physical and chemical systems [41–44], exotic ultraslow logarithmic relaxation extends beyond the scope of the Williams-Watts type and necessitates a novel scheme of random processes.

The random walk characterized by log-aging diffusion, as illustrated in Fig. 1, inherently produces an ultraslow relaxation. We systematically calculate the survival probability across various parameters, striving for a universal scaling form. For enhanced clarity, the scenario of a single defect ($N=1$) is depicted in Fig. 2. The survival probability ϕ as a function of time for a solitary defect undergoing log-aging diffusion in a one-dimensional sys-

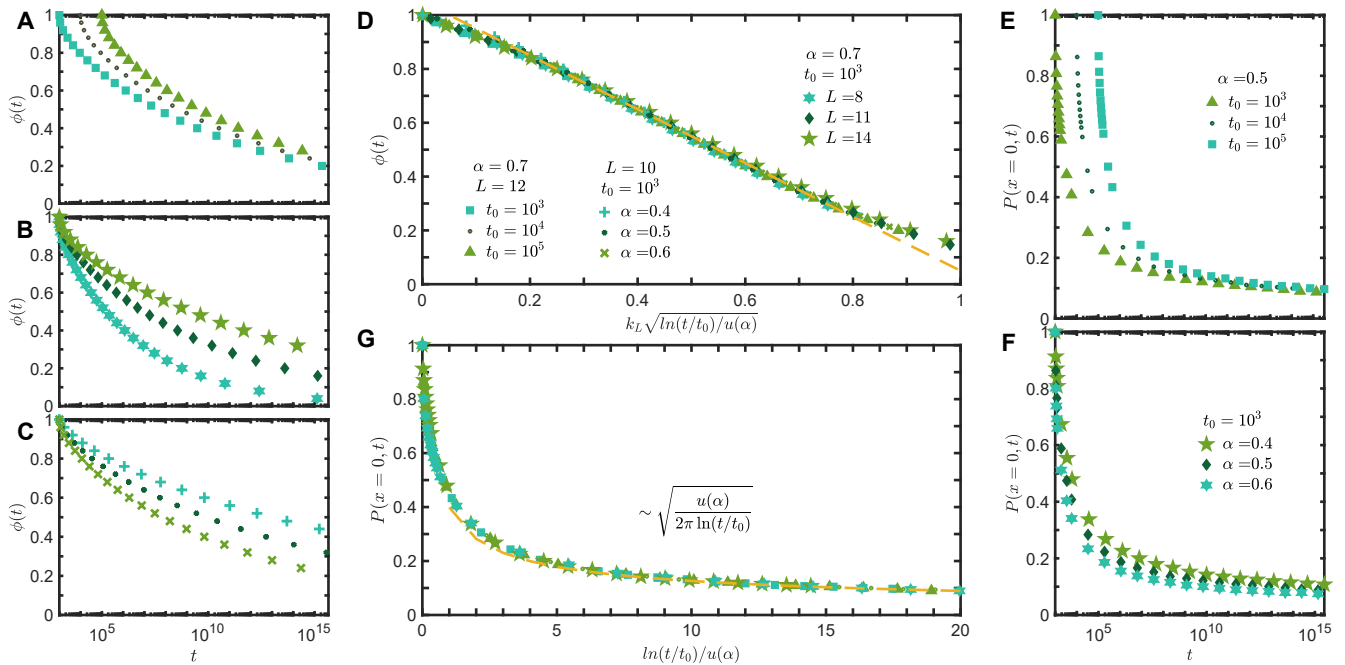


FIG. 2. Survival and returning probability in log-aging diffusion, manifesting universal scaling forms. (A to C), The simulated survival probability ϕ of a single particle on a one-dimensional (1D) lattice is plotted, with length L and lattice spacing $a = 1$. The particle exhibits a log-aging diffusion process with initial time t_0 . (D), The survival probability data from (A to C) are appropriately scaled following Eq. 2, with consistency in the symbolic representation across these sections. In panels (A to D), the same symbol denotes identical parameter values. (E and F), The simulation also explores the returning probability $P(x = 0, t)$ for the particle initially positioned at the origin at time t_0 , providing insights into its likelihood to return to the starting point over time. (G), Data from Sections (E to F) undergo scaling as Eq. 3, maintaining uniformity in symbol usage throughout the analysis. In panels (E to G), the same symbol denotes identical parameter values.

tem, spanning from 0 to 10^{15} (Fig. 2A-C in a log-linear scale), unveils a distinctly ultraslow decay process. Our studies have established that the initial time t_0 , system size L , and the exponent α of the waiting time distribution significantly modulate the non-renewal log-aging random walk and, consequently, the survival probability. In Fig. 2A, the effect of t_0 is pronounced in the short-time regime but converges over the long-time scale, indicating that the decay pattern of survival probability eventually becomes independent of t_0 . Fig. 2B elucidates the correlation between system size L and the rate of decay process, demonstrating that larger systems exhibit slower relaxation rates. Additionally, Fig. 2C portrays how varying the waiting time distribution exponent α influences the rate of decay, revealing that lower values of α correlate with a more gradual decrease in survival probability.

The survival probability across varied scenarios consistently exhibits ultraslow relaxation, as depicted on the log-linear scale in Fig. 2A-C. However, universal characteristics underlying these data are still desirable. Through asymptotic analysis detailed in the Supplement Materials, we have derived the asymptotic form of the survival probability for a single defect undergoing a non-

renewal log-aging random walk:

$$\phi(t) \sim 1 - \frac{1}{L} \sqrt{\frac{8}{\pi}} \left(\frac{\ln t/t_0}{u(\alpha)} \right)^{1/2}. \quad (2)$$

Leveraging this analytical result, we configure the x-axis as: $\frac{1}{L} \sqrt{\frac{8}{\pi}} \left(\frac{\ln t/t_0}{u(\alpha)} \right)^{1/2}$, facilitating a coherent scaling form of the scattered data illustrated in Fig. 2D. Further, the survival probability for N defects, with density $c = \frac{N}{L}$, conforms to the scaling form: $\phi(t) \sim e^{-c \sqrt{\frac{8 \ln t/t_0}{\pi u(\alpha)}}}$. Simulations for N defects are showcased in Fig. S1. This formulation of the survival probability in the log-aging diffusion provides an explanatory basis for the log-aging decay observed in glass systems [2] (see Supplement Materials and Fig. S2).

The ultraslow relaxation characteristic prominently influences the return probability $P(x = 0, t)$, offering profound insights into the diffusion dynamics of defects. As demonstrated in Fig. 2E-F, simulation results for log-aging diffusion in a one-dimensional infinite system, originating at the origin, reveal that $P(x = 0, t)$ decays ultraslowly over extended time periods. Although the initial time t_0 and the exponent α affect the decay rate, their impact converges to consistent behavior over the long term.

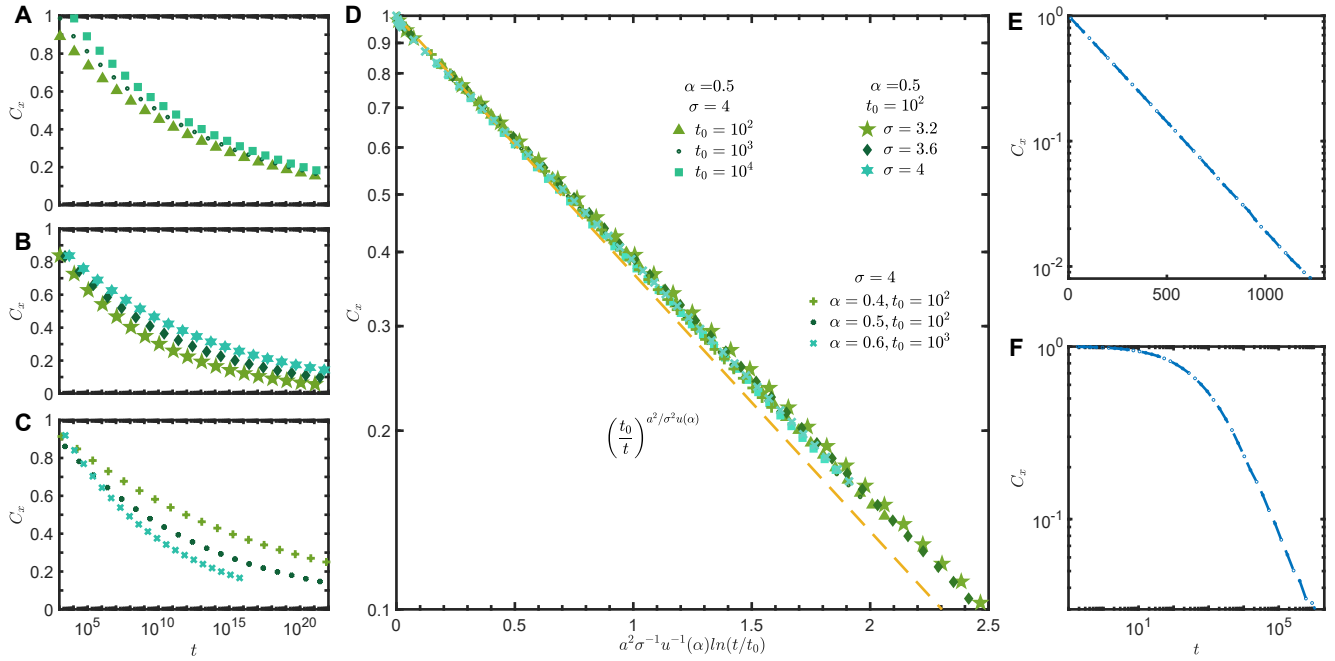


FIG. 3. Scheme and characteristics of log-aging diffusion. **(A)**, We present a log-aging diffusion process, using a scenario where a passenger is waiting to board a bus. The intervals between bus departures at each stop are modeled by a long-tail distribution, expressed as $\psi_\alpha \sim \frac{1}{t^{1+\alpha}}$. Upon the passenger's arrival at the $n-1$ stop, they encounter a wait of t_{n-1} . Once the immediate bus arrives at the $n-1$ stop, the passenger boards swiftly and proceeds to the next stop n with the travel time considerably shorter than the waiting time. Upon reaching stop n , the passenger waits for the next bus, timing the wait as t_n . **(B)**, Displayed are the first nine states of a particle undergoing the diffusion process described in (A), parameterized by $\alpha = 0.6$, $t_0 = 10^3$. We define $u(\alpha) = -\gamma - \partial \ln \Gamma(\alpha) / \partial \alpha$, where γ is the Euler constant and Γ is complete gamma function. **(C)**, The return probability without external forces for the log-aging diffusion is computed as $P(x=0, t)$. **(D)**, The positional autocorrelation function under the influence of an oscillator potential is given, $C_x = \langle x(t)x(0) \rangle$.

From our asymptotic analysis, we deduce the returning probability as follows:

$$P(t) \sim \frac{1}{\sqrt{2\pi} u^{-1}(\alpha) \ln t / t_0}. \quad (3)$$

This formula indicates that the returning probability adheres to a universal scaling form, illustrated in Fig. 2G. For comparison, the asymptotic behavior of subdiffusion over extended durations is expressed by $P(t) \sim \frac{1}{\Gamma(1-\alpha/2)t^{\alpha/2}}$, highlighting a fundamental contrast with log-aging diffusion [18].

Upon analyzing the functional forms of the survival probability, ϕ , and the returning probability, $P(x=0, t)$, we observe that both quantities for the log-aging diffusion are expressible as functions of logarithmic time, $\ln(t/t_0)$, while for subdiffusion, they adhere to power time functions, t^α . These observations suggest a common underlying mechanism, governed by the number of jump steps, n , that dictates the temporal evolution of the walker in internal time space, independent of the type of diffusion. In these diffusion models, the translation from internal time n to laboratory time t is significantly influenced by the waiting time distribution. The survival probability is

explicitly linked to the number of steps n as $1-\phi \propto \sqrt{n}$ in a one-dimensional system with a single defect, and the return probability is modeled as $P(x=0, t) \propto \frac{1}{\langle x^2 \rangle^{d/2}}$, with $\langle x^2 \rangle \propto \langle n \rangle$. By substituting $\langle n \rangle \sim \ln(t/t_0)$ for log-aging diffusion and $\langle n \rangle \sim t^\alpha$ for subdiffusion. Then, in laboratory time, more complex dynamics manifest in various random processes. Nevertheless, after integral transformation to the internal time space, the dynamics can be unified into a simple form (See Supplement Materials for the details).

ULTRASLOW EVOLUTION REVEALED BY AUTOCORRELATION FUNCTION

The autocorrelation function bridges microscopic phenomena with macroscopic behavior [45]. In the time-dependent Ginzburg-Landau theory (TDGL), fluctuations result in the autocorrelation function of the order parameter that exhibits exponential decay [46]. In critical dynamics, the autocorrelation function shows power-law behavior, reflecting unique dynamic properties under critical conditions [47].

To understand correlation in the log-aging diffusion, we

investigate position-position autocorrelation C_x within a confinement potential $U = \frac{m\omega^2 x^2}{2}$. The particle is restricted to jump only to nearest neighbor lattice sites under detailed balance conditions after initial time t_0 , with lattice spacing $a = 1$. The decay process of C_x is monitored up to $t = 10^{22}$, depicted in Fig. 3A-C on a log-linear scale. In particular, C_x does not approach zero even at these extensive timescales. As shown in Fig. 3A, C_x initially depends on t_0 , but this influence vanishes when $t \gg t_0$. Fig. 3B shows that an increase in the variance σ , defined as $\sigma^2 = \frac{k_B T}{m\omega^2}$, results in a slower decay of C_x . Additionally, Fig. 3C reveals that smaller values of α lead to slower decay rates.

The autocorrelation function in this log-aging diffusion manifests in a scaling form:

$$C_x(t, t_0) \sim \left(\frac{t_0}{t}\right)^{a^2/\sigma^2 u(\alpha)}. \quad (4)$$

After the scaling analysis shown in Fig. S3, one can find a remarkable feature that the autocorrelation adheres to a universal scaling form as depicted in Fig. 3D, characterized by an extremely slow power decay.

The dynamics of log-aging diffusion processes can be modeled using a Generalized Langevin Equation (GLE) with a memory kernel:

$$K(t, t') = \frac{u(\alpha)}{\ln t/t'}, \quad (5)$$

where $t > t'$. The solution of this GLE results in an autocorrelation function that is identical to the scaling form shown in Fig. 3D (See Supplement Materials for detailed derivations). For normal diffusion characterized by $K(t, t') \sim \delta(t - t')$, the autocorrelation decays exponentially (Fig. 3E). In subdiffusion, where $K(t, t') \sim (t - t')^{-\alpha}$, $C_x(t)$ follows a Mittag-Leffler function $C_x(t) = E_\alpha(-t/\tau)^\alpha$, illustrating a transition from exponential to power-law decay over time (Fig. 3F). In numerical simulations, similar random processes as shown in Fig. 1A, with various values of $0 < \alpha < 1$, $1 \leq \alpha < 2$, and $\alpha \geq 2$ account for autocorrelation functions shown in Fig. 3D, Fig. 3F, Fig. 3E, respectively (see Supplement Materials for details).

DISCUSSION

The memory kernel of log-aging diffusion process provides a new perspective on the influences of environment on the system, from the relaxation of two-level system [48, 49] to noise-induced anomalous diffusion [50, 51]. For example, Gaussian white noise is correlated with memoryless Markov processes in normal diffusion, while subdiffusion experiences pink noise due to significant memory effects. For log-aging processes, specific environmental noise is necessary to account for its ultraslow evolution

and pronounced long-time memory. Moreover, the remarkable memory effect within the log-aging diffusion calls for in-depth investigations on the interplay of possible ergodicity breaking [52] and a generalized fluctuation dissipation relation.

* haiwen.liu@bnu.edu.cn

- [1] A. Vaknin, Z. Ovadyahu, and M. Pollak, *Phys. Rev. Lett.* **84**, 3402 (2000).
- [2] V. Orlyanchik and Z. Ovadyahu, *Phys. Rev. Lett.* **92**, 066801 (2004).
- [3] O. Ben-David, S. M. Rubinstein, and J. Fineberg, *Nature* **463**, 76 (2010).
- [4] D. Shohat, Y. Friedman, and Y. Lahini, *Nat. Phys* **19**, 1890 (2023).
- [5] A. Gurevich and H. K upfer, *Phys. Rev. B* **48**, 6477 (1993).
- [6] O. B. Tsiok, V. V. Brazhkin, A. G. Lyapin, and L. G. Khvostantsev, *Phys. Rev. Lett.* **80**, 999 (1998).
- [7] A. Samarakoon, T. J. Sato, T. Chen, G.-W. Chern, J. Yang, I. Klich, R. Sinclair, H. Zhou, and S.-H. Lee, *Proc. Natl. Acad. Sci. U. S. A.* **113**, 11806 (2016).
- [8] E. R. Weeks, J. C. Crocker, A. C. Levitt, A. Schofield, and D. A. Weitz, *Science* **287**, 627 (2000).
- [9] I. L. Morgan, R. Avinery, G. Rahamim, R. Beck, and O. A. Saleh, *Phys. Rev. Lett.* **125**, 058001 (2020).
- [10] E. B. Brauns, M. L. Madaras, R. S. Coleman, C. J. Murphy, and M. A. Berg, *Phys. Rev. Lett.* **88**, 158101 (2002).
- [11] Y. Kaplan, S. Reich, E. Oster, S. Maoz, I. Levin-Reisman, I. Ronin, O. Gefen, O. Agam, and N. Q. Balaban, *Nature* **600**, 290 (2021).
- [12] Z. Ovadyahu, *Phys. Rev. Lett.* **99**, 226603 (2007).
- [13] L. Angelani, R. Di Leonardo, G. Parisi, and G. Ruocco, *Phys. Rev. Lett.* **87**, 055502 (2001).
- [14] B. Rinn, P. Maass, and J.-P. Bouchaud, *Phys. Rev. Lett.* **84**, 5403 (2000).
- [15] A. Amir, Y. Oreg, and Y. Imry, *Proc. Natl. Acad. Sci. U. S. A.* **109**, 1850 (2012).
- [16] M. A. Lomholt, L. Lizana, R. Metzler, and T. Ambj rnsson, *Phys. Rev. Lett.* **110**, 208301 (2013).
- [17] E. W. Montroll and G. H. Weiss, *J. Math. Phys.* **6**, 167 (1965).
- [18] R. Metzler and J. Klafter, *Phys. Rep.* **339**, 1 (2000).
- [19] R. Metzler and J. Klafter, *JJ. Phys. A.* **37**, R161 (2004).
- [20] O. Chepizhko and F. Peruani, *Phys. Rev. Lett.* **111**, 160604 (2013).
- [21] D. S. Lee, N. S. Wingreen, and C. P. Brangwynne, *Nat. Phys* **17**, 531 (2021).
- [22] J.-H. Jeon, M. Javanainen, H. Martinez-Seara, R. Metzler, and I. Vattulainen, *Phys. Rev. X* **6**, 021006 (2016).
- [23] T. Koren, M. A. Lomholt, A. V. Chechkin, J. Klafter, and R. Metzler, *Phys. Rev. Lett.* **99**, 160602 (2007).
- [24] A. Lubelski, I. M. Sokolov, and J. Klafter, *Phys. Rev. Lett.* **100**, 250602 (2008).
- [25] J. Li, X. Zhou, J. Li, L. Che, J. Yao, G. McHale, M. K. Chaudhury, and Z. Wang, *Sci. Adv.* **3**, eaao3530 (2017).
- [26] J. H. P. Schulz, E. Barkai, and R. Metzler, *Phys. Rev. X* **4**, 011028 (2014).
- [27] J. Colmenero, A. Alegria, A. Arbe, and B. Frick, *Phys. Rev. Lett.* **69**, 478 (1992).

- [28] A. Giuntoli and D. Leporini, *Phys. Rev. Lett.* **121**, 185502 (2018).
- [29] Z. W. Wu, W. Kob, W.-H. Wang, and L. Xu, *Nat. Commun.* **9**, 5334 (2018).
- [30] H. W. Lau and K. Y. Szeto, *EPL* **90**, 40005 (2010).
- [31] S. Condamin, O. Bénichou, V. Tejedor, R. Voituriez, and J. Klafter, *Nature* **450**, 77 (2007).
- [32] P. H. von Hippel and O. G. Berg, *Proc. Natl. Acad. Sci. U. S. A.* **83**, 1608 (1986).
- [33] M. Saccone, F. Caravelli, K. Hofhuis, S. Parchenko, Y. A. Birkhölzer, S. Dhuey, A. Kleibert, S. van Dijken, C. Nisoli, and A. Farhan, *Nat. Phys* **18**, 517 (2022).
- [34] A. Keren, P. Mendels, I. A. Campbell, and J. Lord, *Phys. Rev. Lett.* **77**, 1386 (1996).
- [35] A. Keren, F. Gulener, I. Campbell, G. Bazalitsky, and A. Amato, *Phys. Rev. Lett.* **89**, 107201 (2002).
- [36] S.-k. Ma and J. Rudnick, *Phys. Rev. Lett.* **40**, 589 (1978).
- [37] S. Bhattacharya, S. Gupta, and S. Hazra, in *Advanced Spectroscopic Methods to Study Biomolecular Structure and Dynamics*, edited by P. Saudagar and T. Tripathi (Academic, 2023) pp. 105–123.
- [38] E. N. 't Hoen, T. Cremer, R. C. Gallo, and L. B. Margolis, *Proc. Natl. Acad. Sci. U. S. A.* **113**, 9155 (2016).
- [39] S. C. Kou and X. S. Xie, *Phys. Rev. Lett.* **93**, 180603 (2004).
- [40] M. F. Shlesinger and E. W. Montroll, *Proc. Natl. Acad. Sci. U. S. A.* **81**, 1280 (1984).
- [41] C. Mongin, P. Moroz, M. Zamkov, and F. N. Castellano, *Nat. Chem.* **10**, 225 (2018).
- [42] N. Rabiei, S. H. Amirshahi, and M. Haghghat Kish, *Phys. Rev. E* **99**, 032502 (2019).
- [43] H. Teichler, *Phys. Rev. Lett.* **107**, 067801 (2011).
- [44] J. Song, Q. Zhang, F. de Quesada, M. H. Rizvi, J. B. Tracy, J. Ilavsky, S. Narayanan, E. D. Gado, R. L. Leheny, N. Holten-Andersen, and G. H. McKinley, *Proc. Natl. Acad. Sci. U. S. A.* **119**, e2201566119 (2022).
- [45] A. Dechant, E. Lutz, D. A. Kessler, and E. Barkai, *Phys. Rev. X* **4**, 011022 (2014).
- [46] M. Tinkham, *Introduction to superconductivity* (Courier Corporation, 2004) pp. 308–315.
- [47] U. C. Täuber, *Critical dynamics: a field theory approach to equilibrium and non-equilibrium scaling behavior* (Cambridge University Press, 2014) pp. 319–321.
- [48] A. J. Leggett, S. Chakravarty, A. T. Dorsey, M. P. A. Fisher, A. Garg, and W. Zwerger, *Rev. Mod. Phys.* **59**, 1 (1987).
- [49] A. A. Stanislavsky, *Phys. Rev. E* **67**, 021111 (2003).
- [50] K. Agarwal, S. Gopalakrishnan, M. Knap, M. Müller, and E. Demler, *Phys. Rev. Lett.* **114**, 160401 (2015).
- [51] S. Gopalakrishnan, K. R. Islam, and M. Knap, *Phys. Rev. Lett.* **119**, 046601 (2017).
- [52] Y. He, S. Burov, R. Metzler, and E. Barkai, *Phys. Rev. Lett.* **101**, 058101 (2008).

Supplement Materials: The route of random process to ultraslow aging phenomena

Chunyan Li,¹ Haiwen Liu,^{1,2,*} and X. C. Xie^{2,3,4}

¹Center for Advanced Quantum Studies, Department of Physics, Beijing Normal University, Beijing 100875

²Interdisciplinary Center for Theoretical Physics and Information Sciences, Fudan University, Shanghai 200433, China

³International Center for Quantum Materials, School of Physics, Peking University, Beijing 100871, China

⁴Hefei National Laboratory, Hefei 230088, China

SURVIVAL PROBABILITY

The survival probability of a fixed target surrounded by uniform distributed defects is [1, 2]

$$\phi(t) = \left[1 - \frac{1}{L} \int_0^t I(t) dt \right]^N, \quad (1)$$

where N is the number of defects, L is the number of the lattice points, $I(t)$ is the rate of defects visiting new sites firstly.

For defects undergoing log-aging diffusion process,

$$I(t) = \sum_{s \neq 0} \sum_n F_n(s) \rho_n(t),$$

where $\rho_n(t)$ is the probability for the time of execution of j th step, and $F_n(s)$ is the probability of the defect originally at origin firstly reaching at the site s after n steps. According to ref [3], the Mellin transform $(f(p) \equiv \int_0^\infty t^{p-1} f(t) dt)$ of $\rho_n(t)$ is $\rho_n(p) = G^n(p-1) t_0^{p-1}$, where $G(p) \sim 1 + u(\alpha)p$ for small p . Then we denote $P_n(s)$ the probability of the defect originally at origin arriving the site s after n steps and define generating function of $F_n(s)$ and $P_n(s)$, that is $F_z(s, z) \equiv \sum_n F_n(s) z^n$, $P_z(s, z) \equiv \sum_n P_n(s) z^n$. The relation between them is $\sum_{s \neq 0} F_z(s, z) = \frac{1}{(1-z)P_z(0, z)} - 1$. [1] Thus, the Mellin transform of $I(t)$ is

$$I(p) = t_0^{p-1} \left(\frac{1}{u(\alpha)(1-p)P_z(0, 1+u(\alpha)(p-1))} \right) \quad (2)$$

1D results

In simple 1D lattice [4],

$$P_z(0, z) \sim (1 - z^2)^{-1/2}. \quad (3)$$

After substituting Eq. (3) into Eq. (2), it's gotten that

$$I(p) \sim t_0^{p-1} \frac{\sqrt{2}}{\sqrt{u(\alpha)(1-p)}}$$

The inverse Mellin transform of this expression gives asymptotically

$$I(t) = \frac{1}{t_0} \sqrt{\frac{2}{u(\alpha)\pi}} \frac{1}{\frac{t}{t_0} \sqrt{\ln \frac{t}{t_0}}}$$

Consequently, for the case of $N = 1$, the survival probability is given as

$$\phi = 1 - L^{-1} \sqrt{\frac{8 \ln t/t_0}{\pi u(\alpha)}} \quad (4)$$

In limit of large N and large L , but with a constant concentration $\lim_{N, L \rightarrow \infty} \frac{N}{L} = c$,

$$\phi = \exp(-\int I(t) dt) = \exp\left(-c \sqrt{\frac{8 \ln t/t_0}{\pi u(\alpha)}}\right) \quad (5)$$

Simulations with constant c by increasing L gradually are plotted in Fig. S1. It's cleared that they approached a limit function shown by dashed line (according to Eq. (5)).

3D results

When we consider 3D case [4],

$$P_z(0, z) \sim 1.51636 - \frac{3}{\pi} \left(\frac{3}{2}\right)^{1/2}.$$

It's gotten that

$$I(p) \sim t_0^{p-1} \frac{0.659}{u(\alpha)(1-p)}$$

For the case of $N = 1$, the survival probability is given as

$$\phi = 1 - \frac{0.659}{u(\alpha)L} \ln \frac{t}{t_0} \quad (6)$$

Log-aging relaxation has found in Anderson insulator [5, 6], electron glass [7, 8] and other system [9–11]. V. Orlyanchik and Z. Ovadyahu investigated time evolution of conductance, G , of In_2O_{3-x} in the change of field [7]. Firstly, they put a constant stress F_0 through an electric field along a thin film to an steady state, after that, the filed is changed to F much larger than F_0 for a time t_w . Finally, the field was reset to F_0 . Conductance G was measured along the time. After resetting the filed, conductance exhibits a logarithmic slow decay and simple aging, as shown in Fig. S2, $\Delta G \sim A \ln t/t_0$, which is accordant with the behaviour of survival probability of

log-aging diffusion process in 3D Eq. (6). Under a strong field, molecular polarization occurs. The intensity of the field directly correlates with the extent of dipole displacement. The duration, t_w , during which a large field F is applied to an insulator, corresponds to the time t_0 in Eq. (6), representing the duration of environmental application. Due to Anderson localization, impurities are sparsely distributed and thus only affect their nearest polarization. This scenario corresponds to the case of $N = 1$ in a system of size L under the influence of a strong field F .

TIME MATCHING FROM LABORATORY TIME TO INTERNAL TIME

$S(t) = \int I(\tau) d\tau$ is the mean number of distinct visited sites after time t . In discrete jumping steps space, the mean number of distinct sites visited in n steps is [1]

$$S_n = \begin{cases} (8n/\pi)^{1/2} (1D) \\ 0.659n (3D) \end{cases}$$

In continuous laboratory time, we treat n as a continuous variable, and it's natural that

$$S(t) \sim S_{\langle n \rangle} = \begin{cases} (8 \langle n \rangle / \pi)^{1/2} (1D) \\ 0.659 \langle n \rangle (3D) \end{cases}$$

For log-aging case $\langle n \rangle = \frac{\ln t/t_0}{u(\alpha)}$, survival probability ϕ , or no-touching probability, like Eq. (4) or Eq. (5) is obtained as $1 - S_{\langle n \rangle}$. And for normal diffusion and subdiffusion, survival probability is expressed as $S_{\langle n \rangle}$ [1].

In framework of generalized Fokker-Plank equation [12] (LFPE),

$$\int dt' K(t, t') \frac{\partial}{\partial t'} P(x, t') = L_{FP} P(x, t). \quad (7)$$

It can be understood as clocking matching [13] from internal time n to physical time t , $P(x, t) = \int P_0(x, t) h(n, t) dn$, where $P_0(x, n)$ obeys simple normal Fokker-Plank equation in internal time, $h(n, t)$ is the non-linear clocking matching. This matching process produces the memory kernel $K(t, t')$ in LFPE, $K(t, t') \sim \delta(t - t')$ for normal diffusion; $K(t, t') \sim (t - t')^{-\alpha}$ for subdiffusion; $K(t, t') \sim \frac{u(\alpha)}{\ln(t/t')}$ for log-aging diffusion.

AUTOCORRELATION FUNCTION

The generalized Langevin equation [14] is

$$m \frac{d^2 x(t)}{dt^2} = -\zeta \int_{t_0}^t d\tau K(t, \tau) \frac{dx(\tau)}{d\tau} - \frac{dU(x)}{dx} + F(t), \quad (8)$$

where $F(t)$ is the fluctuating force, $K(t, \tau)$ is memory kernel, $U(x)$ is the potential and $\zeta = \frac{m\omega^2\sigma^2}{a^2}$. A differential equation for C_x is obtained by multiplying both sides

of the equation by $x(0)$ and taking the ensemble average, in over-damped limit,

$$m\omega^2 C_x(t) = -\zeta \int_{t_0}^t d\tau K(t/\tau) \frac{dC_x(\tau)}{d\tau}, \quad (9)$$

where $\langle F(t)x(0) \rangle = 0$ [15]. The Mellin transform of Eq. (9) gives

$$C_x(p) = -\frac{C_x(0)t_0^p}{p - \frac{a^2}{\sigma^2} \widehat{K}^{-1}(p)}.$$

Since $\widehat{K}(p) \sim u(\alpha)p^0$, $C_x(p) = -\frac{C_x(0)t_0^p}{p - \frac{a^2}{\sigma^2} u(\alpha)}$. Inverse Mellin transform into time space gives that

$$C_x(t) = C_x(0) \left(\frac{t_0}{t} \right)^{a^2/\sigma^2 u(\alpha)} \quad (10)$$

NUMERICAL SIMULATION

Our stochastic simulations are based on a forward jumping process on a 1D lattice illustrated in Fig. 1A. For survival probability, we simulate the survival probability of uniformed distributed particles not touching absorbing boundaries. For position-position autocorrelation, we simulation N independent particles, under a harmonic oscillator potential $U(x) = \frac{m\omega^2 x^2}{2}$, in a lattice with lattice spacing $a = 1$. Initially, the particles are distributed according to Boltzmann distribution $P(x, 0) \sim \exp(-U(x)/k_B T)$. Forced by harmonic potential force, particles jump to the nearest neighboring point with a transition probability, satisfying the detailed balance condition, $p(x \pm a, x) = \frac{1}{1 + e^{\pm 2ax/\sigma^2}} (\sigma^2 = m\omega^2/k_B T)$. Subsequently, we construct the movement trajectory of each particle, allowing for the calculation of the position autocorrelation function at specific moments in time $C_x = \frac{1}{N} \sum_{i=1}^N x_i(t)x_i(0)$. $\ln(C_x)$ versus $\ln(t/t_0)$ is plotted in Fig. S3A, showing a linear dependence with slope η , depending on the parameter σ and α . As shown in Fig. S3B, when σ increases (approaching to over-damping limit), the slope $\eta = \frac{d \ln C_x}{d \ln t/t_0}$ increases and the ratio of η and a^2/σ^2 eventually reaches a stable value, associated with α . Ultimately, we obtain stable values \widetilde{k} for different α in Fig. S3C and the relation between \widetilde{k} and α is $\widetilde{k} = u^{-1}(\alpha)$. The autocorrelation of different parameters are collapsed in the x-scale of $a^2\sigma^{-2}u^{-1}(\alpha) \ln t/t_0$, as depicted in Fig. 3D in the main text.

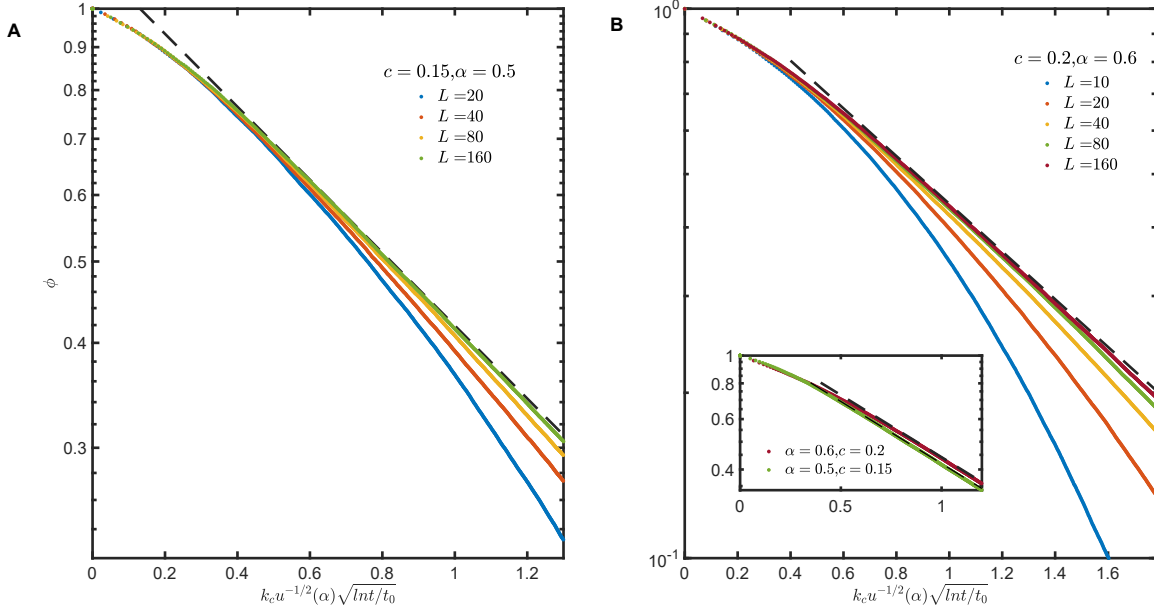


Fig. S 1. Numerical survival probability of the log-aging random defects with a constant concentration. (A), concentration of defects $c = 0.15$ with $\alpha = 0.5$. (B), concentration of defects $c = 0.2$ with $\alpha = 0.6$. Inset: the limit of modification of $L = 160$ of (A) and (B). Dashed lines show the asymptotic behavior of log-aging survival probability with L approaching infinity according to Eq. (2) in the main text.

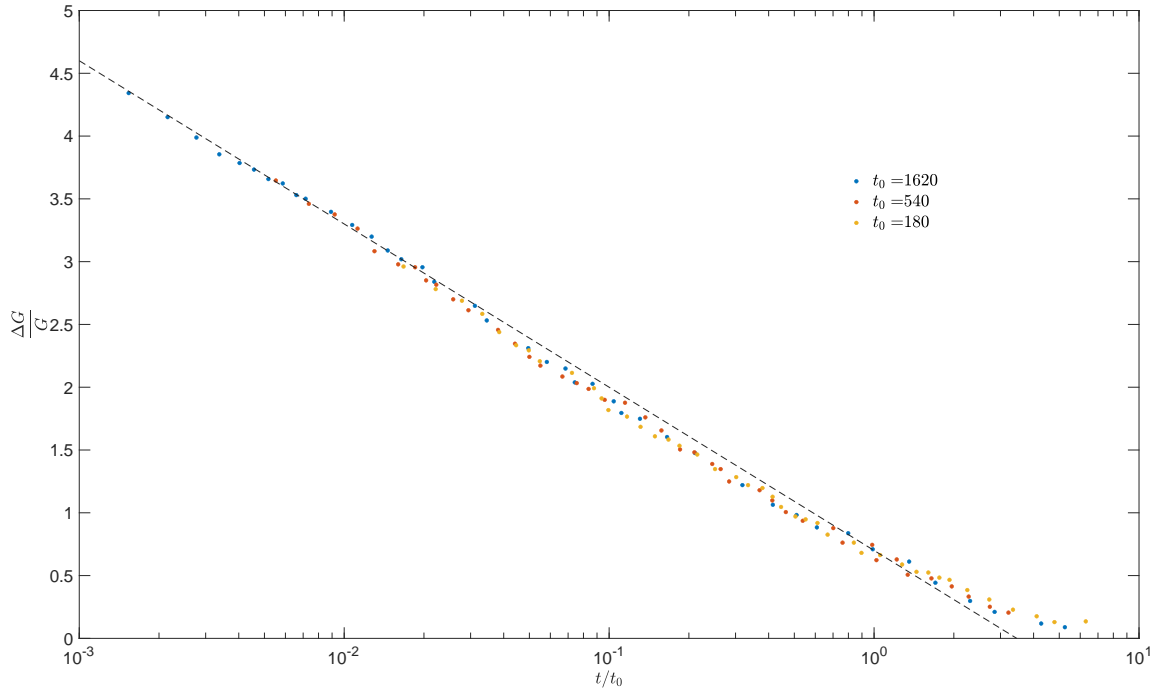


Fig. S 2. Conductance relaxation in Anderson glass follows the survival probability of log-aging defect in 3D medium. A logarithmic relaxation of conductance G in a thin films of In_2O_{3-x} after a sudden change of stress. Data are from Fig.2 in Ref. [7].

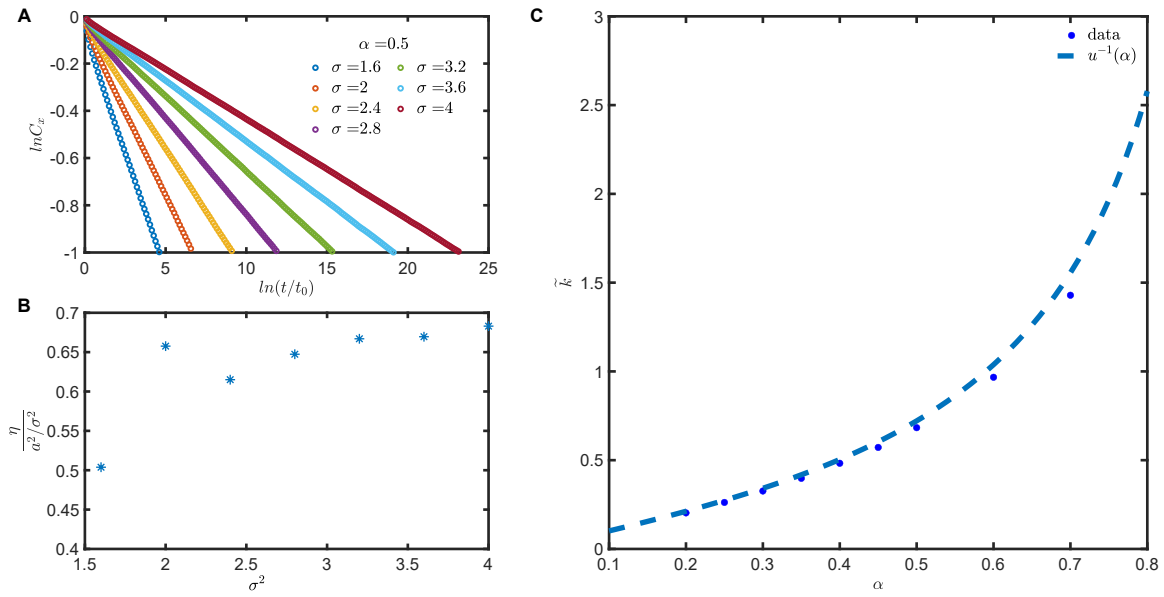


Fig. S 3. **Scaling analysis of numerical results for autocorrelation of log-aging diffusion process.** (A), $\ln(C_x)$ versus $\ln(t/t_0)$ for different values of σ , with $\alpha = 0.5$. There is a linear relationship, $\ln C_x = \eta \ln(t/t_0)$, where η is proportional to $\frac{a^2}{\sigma^2}$. (B), the ratio $\eta/a^2\sigma^{-2}$ versus σ , in the case of $\alpha = 0.5$. It is observed that as σ^2 increases, the ratio $\eta/a^2\sigma^{-2}$ approaches a limit value \tilde{k} . (C), the limiting value $\tilde{k} = \frac{\eta}{a^2/\sigma^2}$ plotted against α , which corresponds to $u^{-1}(\alpha)$.

* haiwen.liu@bnu.edu.cn

- [1] M. F. Shlesinger and E. W. Montroll, *Proc. Natl. Acad. Sci. U. S. A.* **81**, 1280 (1984).
- [2] W. H. Hamill and K. Funabashi, *Phys. Rev. B* **16**, 5523 (1977).
- [3] M. A. Lomholt, L. Lizana, R. Metzler, and T. Ambjörnsson, *Phys. Rev. Lett.* **110**, 208301 (2013).
- [4] E. W. Montroll and G. H. Weiss, *J. Math. Phys.* **6**, 167 (1965).
- [5] Z. Ovadyahu, *Phys. Rev. Lett.* **108**, 156602 (2012).
- [6] A. Vaknin, Z. Ovadyahu, and M. Pollak, *Phys. Rev. Lett.* **84**, 3402 (2000).
- [7] V. Orlyanchik and Z. Ovadyahu, *Phys. Rev. Lett.* **92**, 066801 (2004).
- [8] Z. Ovadyahu and M. Pollak, *Phys. Rev. B* **68**, 184204 (2003).
- [9] D. Shohat, Y. Friedman, and Y. Lahini, *Nat. Phys* **19**, 1890 (2023).
- [10] O. Ben-David, S. M. Rubinstein, and J. Fineberg, *Nature* **463**, 76 (2010).
- [11] K. Matan, R. B. Williams, T. A. Witten, and S. R. Nagel, *Phys. Rev. Lett.* **88**, 076101 (2002).
- [12] T. Sandev, A. Chechkin, H. Kantz, and R. Metzler, *Fract. Calc. Appl. Anal.* **18**, 1006 (2015).
- [13] A. Baule and R. Friedrich, *Phys. Rev. E* **71**, 026101 (2005).
- [14] K. Wang and M. Tokuyama, *Physica A*. **265**, 341 (1999).
- [15] B. J. Berne, J. P. Boon, and S. A. Rice, *J. Chem. Phys.* **45**, 1086 (1966).